Investigation of the $^{10}B(\gamma,p)$ reaction using tagged photons

L. J. de Bever,[1,*] D. Branford,[2] J-O. Adler,[3] B-E. Andersson,[3] I. Bobeldijk,[1] T. Davinson,[2] R. S. Hicks,[4] D. G. Ireland,[2,†] K. Livingston,[2,†] R. L. J. van der Meer,[1,‡] R. A. Miskimen,[4] D. Van Neck,[5] L. Isaksson,[3] R. D. Page,[2,§] G. A. Peterson,[4] J. Rahighi,[2,‖] H. Ruijter,[3] B. Schrøder,[3] G. van der Steenhoven,[1] P. J. Woods,[2] K. Wang,[4,¶] and A. C. Shotter[2]

[1]*Nationaal Instituut voor Kernfysica en Hoge–Energiefysica (NIKHEF), P.O. Box 41882, 1009 DB Amsterdam, The Netherlands*

[2]*Department of Physics and Astronomy, University of Edinburgh, Edinburgh EH9 3JZ, Scotland*

[3]*Department of Nuclear Physics, University of Lund, S-223 62 Lund, Sweden*

[4]*Department of Physics and Astronomy, University of Massachusetts, Amherst, Massachusetts 01003*

[5]*Rijksuniversiteit Gent, Proeftuinstraat 1, Gent, Belgium*

(Received 22 April 1998)

The reaction $^{10}B(\gamma,p)$ has been studied using tagged photons of mean energies $E_\gamma = 57.6$ and 72.9 MeV. Angular distributions and derived single-particle momentum distributions for protons leading to the ground state of ^{9}Be and higher excited states are compared to various calculations made using model parameters constrained by $^{10}B(e,e'p)^9Be$ and $^9Be(p,p')^9Be$ measurements. The effects of varying final-state interactions (including channel couplings) and meson exchange currents are considered. A sizable discrepancy between direct-knockout calculations and the experimental results is observed. If meson exchange currents are included in an approximate fashion, a good description of the $^{10}B(\gamma,p_0)^9Be$ data is found. [S0556-2813(98)05308-4]

PACS number(s): 25.20.−x, 27.20.+n

I. INTRODUCTION

A full understanding of the (γ,p) reaction on nuclei at γ energies between the giant resonances and the onset of pion production ($E_\gamma \sim 50-100$ MeV) still remains at some distance in the future despite vigorous investigations by both experimental and theoretical groups over the last 20 years. The main issue at this time is the relative importance of two-nucleon processes, such as those involving meson exchange currents (MEC's), to direct knockout (DKO) [1–5]. Strong similarities between the (γ,p) and $(e,e'p)$ missing energy spectra, the observed scaling of the (γ,p) cross section with missing momentum, and the forward peaking of the (γ,p) angular distributions have been used previously as arguments in favor of a strong DKO mechanism [3,6,7]. On the other hand, the near equality of (γ,p) and (γ,n) cross sections for light self-conjugate $N=Z$ nuclei [8,9] has been cited as evidence for the importance of two-nucleon processes. Calculations employing the so-called modified quasideuteron (MQD) mechanism [10–12,2] are indeed able to explain the similarity of these cross sections. However, these calculations often fail to reproduce the shapes of the angular distributions and the physical significance of this phenomenological model has been called into question [13]. Other arguments in favor of a nondirect-knockout process include several theoretical calculations of (γ,p) cross sections that give indications of the dominance of MEC contributions in the kinematical domain beyond the giant resonances [14–16,4]. However, recent relativistic calculations for (γ,p) reactions on several nuclei give DKO contributions that are much larger and hence closer to the data than those from nonrelativistic calculations [17,18]. These calculations indicate that MEC effects will not become important until a missing momentum of $p_m = 500$ MeV c^{-1} is reached.

In this paper, we describe a study of the $^{10}B(\gamma,p)$ reaction which was performed to investigate further the two-nucleon contribution to the (γ,p) reaction mechanism. The ^{10}B target was chosen because the $^{10}B(e,e'p)^9Be$ [19,20] and $^9Be(p,p')^9Be$ cross sections [21] are available. Detailed information obtained from these studies on bound-state wave functions, overlap wave functions, spectroscopic factors, and optical model parameters allow the DKO contributions to the cross sections to be calculated more accurately than previously using sophisticated distorted-wave impulse approximation (DWIA) codes developed by the Pavia group [22–24]. Initial calculations of this kind were hampered by the lack of knowledge of the nuclear overlap wave functions and the continuum wave functions of the ejected protons [24]. In our study we have constraints on the bound-state wave functions from the $^{10}B(e,e'p)^9Be$ data and constraints on the continuum wave functions from the $^9Be(p,p')^9Be$ data. This makes our determination of the DKO contributions to the (γ,p) reaction less sensitive to model uncertainties and final-state interactions (FSI's) than is the case for most previous investigations.

II. EXPERIMENTAL METHOD

The experiment was carried out using the tagged photon beam of the MAX-Laboratory [25] at the University of Lund

*Present address: Systor AG, Lautengartenstrasse 6, CH-4002 Basel, Switzerland.

†Present address: Department of Physics and Astronomy, University of Glasgow, Glasgow G12 8QQ, Scotland.

‡Present address: Jefferson Laboratory, Newport News, VA 23606

§Present address: Oliver Lodge Laboratory, University of Liverpool, Liverpool L69 38X, England.

‖Present address: AEOI, NRC, Van de Graaff Laboratory, P.O. Box 11365-8486, Tehran, Iran.

¶Present address: Department of Physics, University of Virginia, Charlottesville, VA 22901.

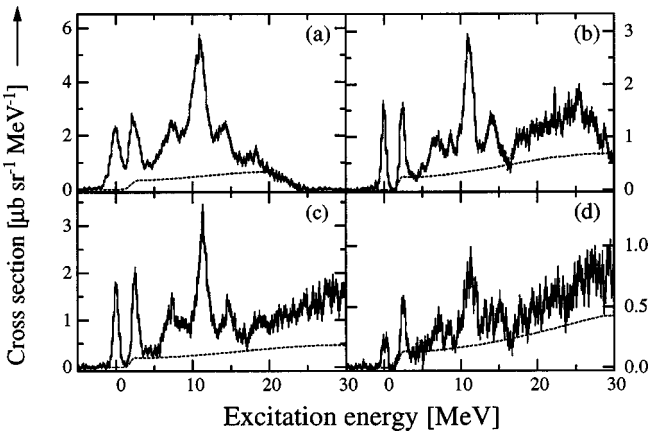

FIG. 1. Cross sections for the ^{10}B(γ,p) reaction. (a) E_γ (θ_p) $=57.6$ MeV (70°), (b) 57.6 (110°), (c) 72.9 (70°), and (d) 72.9 (110°). The dashed lines represent the (γ,np) contribution obtained from a MQD calculation.

in conjunction with a detector arrangement that was very similar to ones that we have reported on previously [26,27]. Bremsstrahlung radiation was generated over two running periods using 50 μm and 160 μm Al radiators in conjunction with electron beams of energies $T_e=75$ MeV and 95 MeV, respectively. The use of an array of 22 plastic scintillator strips in the focal plane of the tagging spectrometer gave rise to tagged photons with energy resolutions of $\sim$330 keV at $T_e=75$ MeV and $\sim$400 keV at $T_e=95$ MeV. The central tagged photon energies were $E_\gamma=57.6$ and 72.9 MeV for the lower and higher T_e, respectively. Tagged photon rates were typically $\sim 3\times10^6$ photons s^{-1}.

A 39 mg cm^{-2} target containing ^{10}B enriched to 92% supported by a 0.89 mg cm^{-2} Kapton backing was placed at $20.0°\pm0.4°$ to the photon beam direction. Knocked out protons were detected in two solid state detector telescopes developed by the nuclear physics group of Edinburgh University [28,29]. Each telescope consisted of two Si strip detectors and a HpGe detector which measured the in-plane emission angles and proton energies, respectively. In total the telescopes covered the angular range $\theta_p=50°-130°$ and subtended a solid angle of 413 ± 20 msr.

As a check on the performance of the system, calibration runs were made using a C target at intervals throughout the experiment. Systematic errors were estimated to be $\sim$ 10% by considering uncertainties associated with the determinations of the tagging efficiency, target thickness, target angle, positions of the detectors, electronic dead times, and losses in the HpGe detectors due to edge effects and nuclear reactions [20]. Within the combined statistical errors and a systematic uncertainty of $\pm10\%$, the ^{12}C$(\gamma,p)^{11}$B results reproduced the known cross sections for transitions to the ground state and first excited state in ^{11}B [30–32]. Hence, a systematic error of $\pm10\%$ is assumed for the results presented here.

III. EXPERIMENTAL RESULTS AND ANALYSES

Figure 1 shows averaged excitation energy spectra obtained with both telescopes after subtracting backgrounds due to the Kapton foils and random events. The mean γ energies quoted are those that correspond to the central electron trajectory of the tagged region in each case. The cross sections are evaluated at a weighted average photon energy; i.e., the photon energy is weighted by both the number of electrons incident on the element and the cross section at that photon energy.

Resolutions of 600–700 keV full width at half maximum (FWHM) were obtained for the ground state and the $E_x=2.41$ MeV peaks shown in Figs. 1(b)–1(d). This is in reasonable agreement with results obtained from Monte Carlo simulations which showed that the main contribution (600 keV) resulted from energy losses in the target. The falloff in the cross section above $E_x\sim25$ MeV for $E_\gamma=57.6$ MeV [see Fig. 1(b)] is due to the signal thresholds on the HpGe detectors. The significantly worse resolution of 1 MeV FWHM obtained for the 70° detector during the $E_x=57.6$ MeV measurement [see Fig. 1(a)] arose because of a malfunction of the detector which precluded operation at the recommended bias voltage. The resulting reduction in the charge collection efficiency also caused an effective cutoff at $E_x\sim19$ MeV as can be seen in Fig. 1(a). However, despite these problems, the test runs made with the C target showed that the detector gave reliable cross sections up to $E_x\sim19$ MeV.

In our analysis, we took account of the fact that the threshold for neutron emission from ^{9}Be is at $E_x=1.665$ MeV. This low threshold gives rise to a continuum under the $E_x=2.41$ MeV and higher excitation peaks due to (γ,np) events where the neutron goes undetected. The dashed lines shown in Fig. 1 are estimates of this background calculated using the MQD code developed by Eden *et al.* [13]. In the calculation, we only considered contributions from the $1p_{3/2}$ orbitals since contributions from deeper orbitals are expected to be significant only at $E_x>20$ MeV [33]. Since the code only provides reliable relative cross sections, the MQD results were fitted to the minima in the spectra at $E_x\sim4$ MeV and ~16 MeV. The results shown in Fig. 1 were obtained using a single normalization factor. As the data displayed in Figs. 1(b)–1(d) can be described by one normalization factor, we feel confident in applying the same factor to Fig. 1(a) where the resolution is insufficient to provide sharp minima at ~4 and ~16 MeV.

Figure 2 shows the angular distribution obtained at $E_\gamma=57.6$ MeV for the ^{10}B$(\gamma,p_0)^9$Be reaction leading to the ground state of ^{9}Be. These results are compared to DWIA calculations made using the Pavia codes [22–24] with different ingredients to investigate the sensitivity of the predicted cross sections to the choice of these ingredients. The bound-state wave functions entering these calculations and the normalization of the curves are fixed by the results of the ^{10}B$(e,e'p)^9$Be analysis [19,20]. Also, the proton final-state interactions are constrained by only using those optical potentials that give a proper description of the ^{9}Be$(p,p')^9$Be data collected at the same proton energy values [21].

First we investigated the sensitivity of the (γ,p) cross sections to the following reaction mechanism aspects [23,24,34–36,9,2]: (1) orthogonality of the initial- and final-state nuclear wave functions, (2) antisymmetrisation of the initial-state nuclear wave function under the exchange of any pair of nucleons, and (3) coupling of the photon to the recoil nucleus. Figure 2(a) shows the results of calculations that

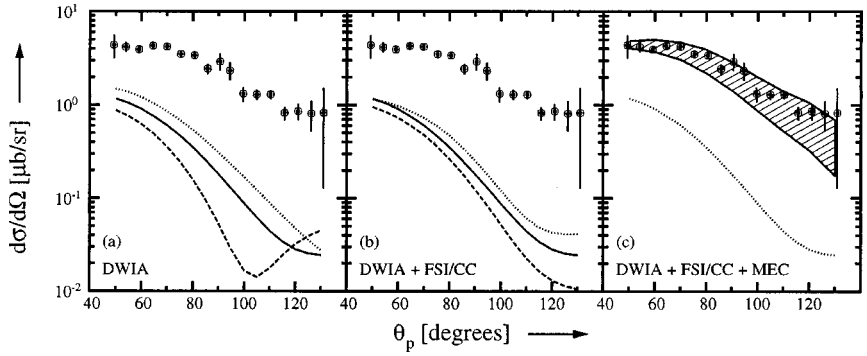

FIG. 2. DWIA calculations compared to the ^{10}B(γ,p_0)^{9}Be results at E_γ=56.7 MeV, which are repeated in graphs (a), (b), and (c), subject to varying the ingredients of the calculations: (a) basic DWIA calculation (dashed line), adding orthogonality and antisymmetrization (solid line), and recoil effects in addition (dotted line); (b) DWIA calculation including orthogonality and antisymmetrization using the SOM optical potential (solid line), reduced CC potential (dashed line), or a full CCIA approach (dotted line); (c) DWIA calculation including orthogonality and antisymmetrization using the SOM optical potential with (solid line) and without (dotted line) MEC correction. The hatched area corresponds to the spread introduced in the calculation by the treatment of the FSI's.

include all three effects (dotted curve), orthogonality and antisymmetrization only (solid curve), and none of these effects (dashed curve). All three calculations employ the same bound-state wave functions for the proton and the same spectroscopic factor $S=0.359$. It is seen that these three effects have a considerable influence on the cross section but do not result in a proper description of the data. In fact the curves lie well below the experimental data at all angles.

Next we studied the sensitivity of the results to FSI's including the effects of explicit channel couplings (CC's) in the final state. These calculations and those discussed later included orthogonality and antisymmetrization corrections but not the coupling of the photon to the residual nucleus. This choice arose from our desire to also consider the effects of MEC's. As both the estimate of MEC's [39] and the coupling of the photon to the residual nucleus [24] involve current conservation, we considered it inappropriate to include both effects simultaneously. The FSI's were obtained using the spherical (SOM) and deformed (reduced CC) phenomenological optical potentials obtained from the ^{9}Be(p,p')^{9}Be measurements [21]. For the coupled-channel calculations, we employed the same coupling scheme as was used in the ^{10}B($e,e'p$)^{9}Be analysis [19,20]. In each of the two types of calculations, the appropriate root-mean-square radius of the bound-state wave function ($r_{\rm rms}$=3.22 and 3.19 fm, respectively) and the spectroscopic factor ($S=0.359$ and 0.365, respectively), as obtained from the ($e,e'p$) analysis, were used.

The results of these calculations are displayed in Fig. 2(b). The solid and dashed curves are DWIA calculations employing the SOM and reduced CC potentials, respectively, whereas the dotted curve was obtained from coupled-channel impulse approximation (CCIA) calculations employing the reduced CC potential for generating both the proton distortions and the channel couplings. Again it is observed that the calculations show a considerable spread, especially at backward angles, and lie well below the experimental data.

The third effect we studied was the contribution due to the MEC's. Here we followed the method first suggested by Ireland and van der Steenhoven [39], which allows an estimate of the contribution from MEC effects to be made in the plane-wave impulse approximation (PWIA) by applying Siegert's theorem. This gave an angle-dependent correction factor by which the results of a standard DWIA calculation were multiplied. As compared to Ref. [39], the method was improved by Van Neck through the inclusion of up to six multipoles (instead of up to $E2$) and removing some mathematical simplifications. The result is shown in Fig. 2(c) as a shaded error band, which represents the uncertainty in the calculation due to FSI's. This uncertainty was determined by considering the spread between the calculations displayed in Fig. 2(c). It is seen that within the errors this correction for MEC effects results in a good description of the data.

Given the success of the MEC correction, it is worthwhile to provide some more details on how this correction factor was actually arrived at. As a starting point, a PWIA calculation was carried out using the same rms radius and spectroscopic factor as before. The FSI's were treated by replacing the missing momentum p_m by an effective momentum $[p_m]_{\rm eff}$ given by $p_p\times(V/T_p)^{1/2}$ with p_p and T_p representing the momentum and kinetic energy of the emitted proton. The average potential V to which the proton was exposed was taken to be 11 MeV for the reasons given below.

The results of this so-called PWIA effective calculation are displayed in Fig. 3(a) (dashed curve). Also included are results using effective charges to account for spurious center-of-mass effects (dotted curve) and MEC effects by applying Siegert's theorem (up to $l=6$) to the single-nucleon current operator (solid curve). Already at this level, a good description of the data is obtained. However, the agreement may be fortuitous because of the seemingly arbitrarily chosen value of $V=11$ MeV. The effect of varying V from 0 to 22 MeV is shown in Fig. 3(b), where a strong dependence of the cross section on V is observed. The value we used for V was deduced from the results of Ref. [21], where it is shown that a Woods-Saxon optical potential with a depth of 22 MeV gives a good description of the ^{9}Be(p,p')^{9}Be data at the same T_p as was used in the present (γ,p) experiment. A proton produced in a ^{10}B(γ,p) experiment will be exposed on average to half the maximum depth of this potential. Hence, $V=11$ MeV is a natural choice, which is supported

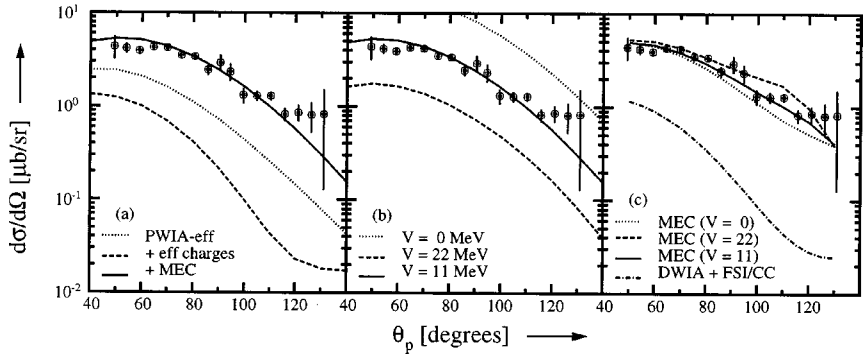

FIG. 3. Estimates of the MEC contribution to the $^{10}\mathrm{B}(\gamma,p_0)^9\mathrm{Be}$ cross section at $E_\gamma=57.6$ MeV. The data are identical to those shown in Fig. 2. In panel (a) the influence of effective charges (dotted line) and the Siegert-theorem-based estimate (solid line) are compared to an effective PWIA calculation (dashed line) and the data. In (b) the influence of the size of the effective FSI potential is studied. In (c) the ratio of these calculations with and without the Siegert operator is applied to the best available DWIA calculation for various values of V.

by Fig. 3(b) where it is seen that this value of V gives the best description of the data.

Figure 3(c) shows results based on MEC correction factors deduced from the results shown in Fig. 3(b). The MEC correction factors were evaluated by taking ratios of the curves displayed divided by the calculations without the Siegert operator at the same V. The resulting ratios were multiplied by the DWIA+FSI/CC curve of Fig. 2(c) [also shown in Fig. 3(c)]. The resulting three curves (dashed for $V=0$, solid for $V=11$, and dotted for $V=22$ MeV) have only a weak dependence on the chosen value of V. This spread is considerably smaller than that due to the uncertainty in the treatment of FSI effects in DWIA calculations as shown in Fig. 2(b). Hence, we feel confident that a reliable estimate of MEC effects for the reaction $^{10}\mathrm{B}(\gamma,p)$ has been obtained which is not strongly dependent on the size of the FSI's. It is noted that fully consistent calculations including FSI's, MEC's, and nuclear structure effects in one framework do not exist for $^{10}\mathrm{B}(\gamma,p)$ due to the complicated nuclear structure of $^{10}\mathrm{B}$. However, such calculations are available for $^{16}\mathrm{O}(\gamma,p)$, confirming the conclusions of our present approximate approach [37,38].

Comparisons between experimental and calculated angular distributions for the other $1p$ transitions observed in the $^{10}\mathrm{B}(\gamma,p)$ spectrum were performed in a similar fashion to those for the ground-state transition. The results are shown in Fig. 4. In each case we used the rms radius of the bound-state wave function and the spectroscopic factor as obtained from the $^{10}\mathrm{B}(e,e'p)^9\mathrm{Be}$ analysis [19,20]. The dotted curves represent the (γ,np) contribution calculated with the MQD code [13] and the shaded error bands represent the incoherent sum of the MQD and DWIA calculations including uncertainties in the FSI's. It is observed that the results for all the $1p$ transitions above the two-nucleon emission threshold are very similar in shape. At both $E_\gamma=57.6$ MeV and 72.9 MeV, it is seen that the incoherent sum of single-nucleon and two-nucleon knockout contributions underestimate the data by a factor of 2–3. The calculated results do have the correct slope, however. Only at extreme backward angles are the calculations close to the data, which is mainly due to the two-nucleon contribution.

To consider the $^{10}\mathrm{B}(\gamma,p)$ data further, we made a comparison to the $^{10}\mathrm{B}(e,e'p)^9\mathrm{Be}$ data in terms of reduced cross sections. Momentum density distributions were obtained from the (γ,p) data using the plane-wave impulse representation of the cross section that neglects FSI's [6]. The results are compared to the reduced cross sections for the $^{10}\mathrm{B}(e,e'p)^9\mathrm{Be}$ data [20] in Fig. 5. Since the results are

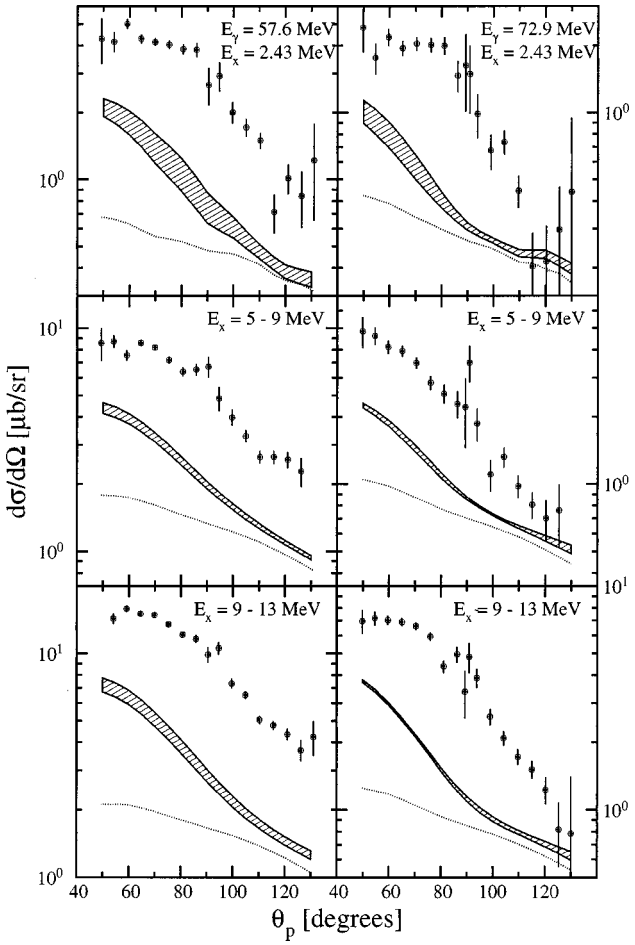

FIG. 4. Angular distributions of the $^{10}\mathrm{B}(\gamma,p)$ reaction at $E_\gamma=57.6$ MeV (left panel) and 72.9 MeV (right panel). The dotted curves (solid curves) are MQD (DWIA + incoherent MQD) results. The shaded error bands arise from a consideration of the uncertainties in FSI's. The normalization of the DWIA curves is fixed by the $^{10}\mathrm{B}(e,e'p)^9\mathrm{Be}$ data.

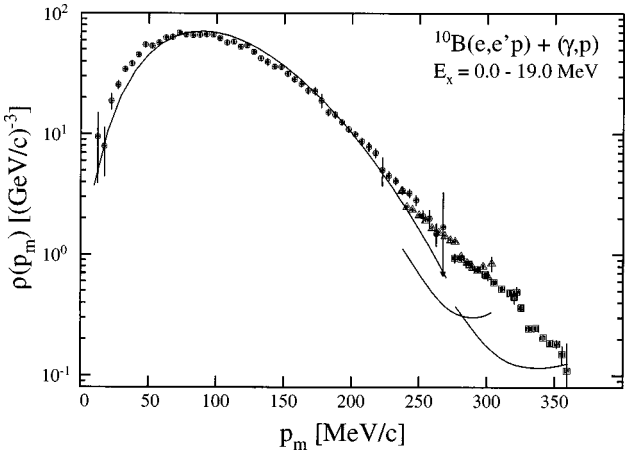

FIG. 5. Reduced cross sections of the ^{10}B($e,e'p$)^{9}Be (circles) and ^{10}B(γ,p) reactions [triangles (57.6 MeV) and squares (72.9 MeV)], integrated over the experimentally accessible $1p$ knockout strength. The solid curves represent DWIA calculations employing the nuclear overlap wave function derived from ^{10}B($e,e'p$)^{9}Be data. In the (γ,p) case the curves include an incoherent MQD contribution due to two-nucleon knockout.

qualitatively the same for all $1p$ transitions, only the comparison of the integrated $1p$ knockout is shown. We observe a smooth connection between the ($e,e'p$) and (γ,p) data which is similar to that reported for ^{12}C and ^{16}O [40,7,39]. However, as the data sets were taken under very different kinematical conditions, the energy of the ejected proton in both reactions differs by about 70 MeV, which results in different amounts of absorption in the final state. Hence, in the DKO framework a smooth connection is not expected. The solid lines show DWIA results obtained using the overlap wave functions and FSI optical model parameters fixed by ^{10}B($e,e'p$)^{9}Be and ^{9}Be(p,p')^{9}Be data. A two-nucleon knockout contribution obtained from the MQD calculation was incoherently added to the DWIA results for the (γ,p) reaction. Similarly to the findings for the angular distributions, we observe that the calculations underestimate the (γ,p) data by a factor of 2–3. This is a clear indication that the (γ,p) reaction using tagged photons cannot be simply used as a probe of the high momentum part of the single-nucleon wave function. However, it can also be concluded that most of the strength observed in (γ,p) in this energy domain most likely can be attributed to MEC's. This conclusion has already been investigated in followup experiments on heavier nuclei which suggest that the effects of MEC's decrease with increasing target mass [41].

It is of interest to note that relativistic calculations [17,18] are able to provide a much better description of (γ,p) data in the energy domain of our ^{10}B(γ,p) measurement than the nonrelativistic DKO calculations presented here. However, one should be cautious of comparing the results of relativistic and nonrelativistic calculations as almost all ingredients are different. For example, the bound-state wave function used in the relativistic calculations is derived from relativistic Hartree potentials, of which only the normalization is adjusted to reproduce existing ($e,e'p$) data. Hence the radius is fixed, whereas it is known [19] that the radius to be used for a proper description of the ^{10}B($e,e'p$)^{9}Be results differs markedly from the one commonly taken from (e,e') data. This may affect the calculated ^{10}B(γ,p) cross sections significantly. Dirac phenomenological optical potentials were used to estimate FSI's. For the ^{10}B(γ,p) calculations, these potentials were obtained by interpolation [18], whereas the standard optical potentials used here are based on a detailed study of a large collection of ^{9}Be(p,p')^{9}Be data [21]. It may be highly questionable to use interpolated Dirac potentials at such low energies, where Ref. [21] shows that a very subtle tuning of the optical model parameters is needed before an adequate description of the proton scattering data is found. A final point to note is that the appropriate relativistic (i.e., no nonrelativistic reduction) current operator has been used. As a result part of the exchange currents may already be effectively absorbed in the use of this more appropriate current operator. Although it is tempting to believe that the last point is likely to explain most of the observed differences between the relativistic and nonrelativistic approaches, it is clear that the input of the relativistic (γ,p) calculations concerning the bound-state wave function and the optical potential needs to be brought to the same level of precision before such far-reaching conclusions can be drawn.

IV. CONCLUSIONS

A detailed analysis of the ^{10}B(γ,p) data has been presented in an effort to study the relative importance of direct knockout and MEC contributions in the intermediate energy domain of $50 \leqslant E_\gamma \leqslant 100$ MeV. Our results show that in order to obtain a reasonable estimate of the DKO contribution to the ^{10}B(γ,p) cross section it is necessary to have a detailed knowledge of the overlap wave functions (i.e., the rms radius and the spectroscopic factor) and the FSI's. Here we have carried out DKO calculations in a nonrelativistic framework constrained by the results of ^{10}B($e,e'p$)^{9}Be and ^{9}Be(p,p')^{9}Be measurements. Even with these constraints there still remain considerable uncertainties in the DKO estimates. However, as the resulting curves all fall short of the (γ,p) data by a factor of 2–10, the results suggest that processes other than DKO such as MEC effects play a far more crucial role in the (γ,p) reaction. A careful estimate of the MEC contribution to the ^{10}B(γ,p) cross section yields a good description of the data, showing the dominance of MEC effects in this energy domain. These results confirm the findings of Ref. [39] on other nuclei. However, our conclusions are not confirmed by the results of relativistic calculations in their present form. It has to be argued that the input constraints imposed on the relativistic calculations should be brought to the same level of precision as is presently available in the nonrelativistic framework before further conclusions can be drawn.

ACKNOWLEDGMENTS

We wish to thank the staff of the MAX-Laboratory for the smooth operation of the accelerator. The support of the Swedish National Science Research Council is gratefully acknowledged as well as the support of the Kurt and Alice Wallenberg Foundation, the Crafoord Foundation, and the Swedish Institute and the contribution from the Royal Swed-

ish Academy of Sciences. The support of the UK Science and Engineering Research Council is gratefully acknowledged. This work is part of the research program of the FOM-institute for subatomic physics, NIKHEF, which is financially supported by the Netherlands' Organization for Scientific Research (NWO). This work was supported in part by grants from the U.S. Department of Energy and National Science Foundation.

[1] M.J. Leitch, J.L. Matthews, W.W. Sapp, C.P. Sargent, S.A. Wood, D.J.S. Findlay, R.O. Owens, and B.L. Roberts, Phys. Rev. C **31**, 1633 (1985).
[2] M.R. Sené, I. Anthony, D. Branford, A.G. Flowers, A.C. Shotter, C.H. Zimmerman, J.C. McGeorge, R.O. Owens, and P.J. Thorley, Nucl. Phys. **A442**, 215 (1985).
[3] J.L. Matthews, in *Proceedings of the Third Workshop on Perspectives in Nuclear Physics at Intermediate Energies*, ICTP, Trieste, 1987, edited by S. Boffi, C. Ciofi degli Atti, and M. Giannini (World Scientific, Singapore, 1988), p. 611.
[4] J. Ryckebusch, K. Heyde, D. Van Neck, and M. Waroquier, Phys. Lett. B **216**, 252 (1989).
[5] B. Höistad, E. Nilsson, J. Thun, S. Dahlgren, S. Isaksson, G.S. Adams, C. Landberg, T.B. Bright, and S.R. Cotanch, Phys. Lett. B **276**, 294 (1992).
[6] D.J.S. Findlay and R.O. Owens, Phys. Rev. Lett. **37**, 674 (1976).
[7] D.J.S. Findlay, R.O. Owens, M.J. Leitch, J.L. Matthews, C.A. Peridier, B.L. Roberts, and C.P. Sargent, Phys. Lett. **74B**, 305 (1978).
[8] H. Schier and B. Schoch, Nucl. Phys. **A229**, 93 (1974).
[9] M.R. Sené, I. Anthony, D. Branford, A.G. Flowers, A.C. Shotter, C.H. Zimmerman, J.C. McGeorge, R.O. Owens, and P.J. Thorley, Phys. Rev. Lett. **50**, 1831 (1983).
[10] J.S. Levinger, Phys. Rev. **84**, 43 (1951).
[11] B. Schoch, Phys. Rev. Lett. **41**, 80 (1978).
[12] B. Schoch, H. Göringer, P. Jennewein, F. Klein, G. Lührs, and F. Zettl, Phys. Rev. C **22**, 2630 (1980).
[13] J.A. Eden *et al.*, Phys. Rev. C **44**, 753 (1991).
[14] M. Gari and H. Hebach, Phys. Rep. **72**, 1 (1981).
[15] J. Ryckebusch, M. Waroquier, K. Heyde, and D. Ryckbosch, Phys. Lett. B **194**, 453 (1987).
[16] J.P. McDermott, E. Rost, J.R. Shepard, and C.Y. Cheung, Phys. Rev. Lett. **61**, 814 (1988).
[17] J.I. Johansson, H.S. Sherif, and G.M. Lotz, Nucl. Phys. **A605**, 517 (1996).
[18] J.I. Johansson and H.S. Sherif, Phys. Rev. C **56**, 328 (1997).
[19] L.J. de Bever *et al.*, Phys. Rev. Lett. **80**, 3924 (1998).
[20] L.J. de Bever, Ph.D. thesis, University of Utrecht, 1993.
[21] L.J. de Bever *et al.*, Nucl. Phys. **A579**, 13 (1994).
[22] S. Boffi, C. Giusti, and F.D. Pacati, Nucl. Phys. **A359**, 91 (1981).
[23] S. Boffi, F. Cannata, F. Capuzzi, C. Guisti, and F.D. Pacati, Nucl. Phys. **A379**, 509 (1982).
[24] S. Boffi, R. Cenni, C. Guisti, and F.D. Pacati, Nucl. Phys. **A420**, 38 (1984).
[25] J-O. Adler *et al.*, Nucl. Instrum. Methods Phys. Res. A **294**, 15 (1990).
[26] D.G. Ireland *et al.*, Nucl. Phys. **A554**, 173 (1993).
[27] I. Bobeldijk *et al.*, Phys. Lett. B **356**, 13 (1995).
[28] A.C. Shotter, S.V. Springham, D. Branford, J. Yorkston, J.C. McGeorge, B. Schoch, and P. Jennewein, Phys. Rev. C **37**, 1354 (1988).
[29] S.V. Springham *et al.*, Nucl. Phys. **A517**, 93 (1990).
[30] J.L. Matthews, D.J.S. Findlay, S.N. Gardiner, and R.O. Owens, Nucl. Phys. **A267**, 51 (1976).
[31] J.C. McGeorge *et al.*, Phys. Lett. B **179**, 212 (1986).
[32] H. Ruijter *et al.*, Phys. Rev. C **54**, 3076 (1996).
[33] J. Mougey, M. Bernheim, A. Bussière, A. Gillebert, Phan Xuan Ho, M. Priou, D. Roger, I. Sick, and G.J. Wagner, Nucl. Phys. **A262**, 461 (1976).
[34] R.D. Amado, F. Cannata, and J.P. Dedonder, Phys. Rev. C **31**, 162 (1985).
[35] R. Cenni and G.A. Rottigni, Lett. Nuovo Cimento **15**, 574 (1976).
[36] C. Ciofi degli Atti, M.M. Giannini, and G. Salmè, Nuovo Cimento A **76**, 225 (1983).
[37] J. Ryckebusch, M. Waroquier, K. Heyde, J. Moreau, and D. Ryckbosch, Nucl. Phys. **A476**, 237 (1988).
[38] J. Ryckebusch, K. Heyde, L. Machenil, D. Ryckbosch, M. Vanderhaegen, and M. Waroquier, Phys. Rev. C **46**, R829 (1992).
[39] D.G. Ireland and G. van der Steenhoven, Phys. Rev. C **49**, 2182 (1994).
[40] D.J.S. Findlay and R.O. Owens, Nucl. Phys. **A292**, 53 (1977).
[41] E.C. Aschenauer *et al.*, Nucl. Phys. **A615**, 33 (1997).